Biophysical Journal Volume 101 October 2011 1781–1787

Characterization of Enhanced Monovalent and Bivalent Thrombin DNA Aptamer Binding Using Single Molecule Force Spectroscopy

Isabel Neundlinger,[†] Alexandra Poturnayova,[‡] Ivana Karpisova,[§] Christian Rankl,[¶] Peter Hinterdorfer,[†‖**] Maja Snejdarkova,[‡] Tibor Hianik,[§] and Andreas Ebner[†*]

[†]Biophysics Institute, Johannes Kepler University Linz, Linz, Austria; [‡]Institute of Biochemistry and Animal Genetics, Slovak Academy of Sciences, Ivanka pri Dunaji, Slovakia; [§]Faculty of Mathematics, Physics and Informatics, Comenius University, Bratislava, Slovakia; [¶]Agilent Technologies, Austria GmbH, Linz, Austria; [‖]Center for Advanced Bioanalysis, Linz, Austria; and **Christian Doppler Laboratory for Nanoscopic Methods in Biophysics, Biophysics Institute JKU, Linz, Austria

ABSTRACT Thrombin aptamer binding strength and stability is dependent on sterical parameters when used for atomic force microscopy sensing applications. Sterical improvements on the linker chemistry were developed for high-affinity binding. For this we applied single molecule force spectroscopy using two enhanced biotinylated thrombin aptamers, BFF and BFA immobilized on the atomic force microscopy tip via streptavidin. BFF is a dimer composed of two single-stranded aptamers (aptabody) connected to each other by a complementary sequence close to the biotinylated end. In contrast, BFA consists of a single DNA strand and a complementary strand in the supporting biotinylated part. By varying the pulling velocity in force-distance cycles the formed thrombin-aptamer complexes were ruptured at different force loadings allowing determination of the energy landscape. As a result, BFA aptamer showed a higher binding force at the investigated loading rates and a significantly lower dissociation rate constant, k_{off}, compared to BFF. Moreover, the potential of the aptabody BFF to form a bivalent complex could clearly be demonstrated.

INTRODUCTION

Noncovalent interactions are known to play a central role in a lot of biological processes. Here, usually ligand-receptor complexes of proteins (e.g., antibodies, enzymes) and/or other organic biomolecules (e.g., vitamins, hormones) are formed. Although the stability of these biomolecules is optimized for its biological application, in vitro measurements can be significantly limited by denaturation processes. In the last decade a large number of DNA or RNA aptamers has been developed showing a high affinity to a certain number of biological binding partners. By using the systematic evolution of ligands by exponential enrichment approach (1) the number of newly developed aptamers is still growing. The aptamers are usually constructed of a single-stranded nucleic acid chain forming a structure perfectly fitting into the binding pocket of its corresponding ligand. The very high stability of DNA in combination with sufficient affinity allows the substitution of denaturable proteins (e.g., antibodies), especially in applications where long-term stability is needed. Since their discovery in 1989 (1) the aptamers are of increased interest as receptors in affinity biosensors (2) or for targeted drug delivery and therapy (3). Among DNA aptamers those sensitive to thrombin are best investigated. Thrombin is a multifunctional serine protease that plays an important role in procoagulant and anticoagulant functions. Thrombin converts soluble fibrinogen to insoluble fibrin that forms the fibrin gel, which is responsible either for a physiological plug or for pathological thrombus (4). Therefore, the first DNA aptamers selective to the fibrinogen binding site at thrombin has been developed as an anticoagulant to prevent the formation of thrombus (5). The structural motif of these aptamers consists of 15 nucleotides that form a guanine quadruplex (G-quadruplex) stabilized by intramolecular hydrogen bonds (6). These aptamers have been used in many studies as a receptor for recognition of thrombin (see (7) for review). In addition to high stability the important advantage of DNA aptamers is a relatively easy modifiability by various chemical groups, such as biotin or thiols, allowing them to be immobilized at various surfaces. This makes aptamers promising candidates for biosensing atomic force microscopy (AFM) techniques such as single molecule force spectroscopy (SMFS) or recognition imaging. SMFS (8–12), enables the exploration of the energy landscape on a molecular level. For this purpose, the AFM tip has to be functionalized with a well-adjusted surface density, resulting in statistically only one ligand at the outer apex of the tip (10,13–15). This monomolecular biosensor tip is then repeatedly brought into contact with a surface containing its corresponding receptor. Since both, the tethering of the ligand as well as the measurement itself usually takes a couple of hours, the lifetime of the ligand can be limiting for the whole process. The use of DNA aptamers as a ligand substitute on the AFM tip overcomes this limitation resulting in sensors stable for weeks or even longer. First approaches using aptamer biosensor tips have shown their potential in SMFS (16,17) as well as in recognition

Submitted February 28, 2011, and accepted for publication July 28, 2011.

*Correspondence: Andreas.Ebner@jku.at

Andreas Ebner's present address is Biophysics Institute, Johannes Kepler University Linz, Linz, Austria.

Editor: Catherine A. Royer.

0006-3495/11/10/1781/7 $2.00

doi: 10.1016/j.bpj.2011.07.054

imaging (18). Earlier studies on DNA modified AFM tips demonstrated the ability to measure single DNA-protein interaction forces. In particular, Basnar et al. (16) used thiolated DNA aptamers selective to the fibrinogen binding site of thrombin at a gold-coated AFM tip and studied the interaction of these aptamers with thrombin molecules covalently attached to gold slides. They reported surprisingly low rupture forces for a thrombin-aptamer complex of ~4.45 pN, which are supposed to correspond to the melting of G-quadruplexes. However, previous studies in which the interaction between DNA-fragments and DNA-binding peptides and proteins was investigated revealed at least 10 times higher forces (19,20). Bartels et al. (21), for example, measured rupture forces of 50–165 pN at loading rates of 70–79 000 pN/s between an AFM tip coupled *exp* promoter DNA fragment encoding proteins required for generation of bacterial exopolysaccarides and its corresponding transcriptional activator protein ExpG. Thus, it might be that the dense coverage of the aptamers on the AFM tip causes difficulties in optimal binding to the thrombin. Therefore, the development of a more efficient system based on single aptamer modification of the AFM tip is required.

The sterical design of the AFM aptamer tips plays a critical role in the stability of the interaction. Using the same ligand-receptor pair but with an inverted system Yu et al (22) showed a significantly stronger complex formation compared to Basnar et al. (16) by sensing a DNA aptamer functionalized surface with a thrombin tethered on the tip. The arrangement of Yu (22) avoids sterical problems and results in optimal conditions for complex formation. Within this study we show how to overcome the limitations when using enhanced linker design for aptamer immobilization design on the sensing tip. So far, mostly the conventional single-stranded DNA aptamers were used in molecular recognition studies. It has been shown, that the binding affinity between aptamers and proteins can be substantially increased by aptamer dimers formed either by linking two single-stranded aptamers by ligase (23) or by hybridization of aptamers supporting parts (24). The new term "aptabody" has been introduced for aptamer dimers (24). The potentiality of bivalent binding of aptabodies brings a substantial advantage, because it can increase the binding effectivity of the aptamer dimer to the corresponding ligand. It has been shown that engineered aptamers like multivalent circular constructs exhibit increased stability against cleavage by exonucleases and improved (2–3-fold) anticoagulant activity in comparison with conventional single-stranded aptamers (25). In recent experiments we were able to show that aptamer homodimers selective to the fibrinogen binding site of thrombin causes a twofold decrease of the ability of thrombin to cleave fibrinogen (26). Thus, the aptabody can serve as a more effective anticoagulant in comparison with conventional single-stranded aptamers. Increased inhibitory activity against HIV-1 reverse transcriptase has also been shown for lately reported bimodular DNA aptamers (27).

Recently, the detailed study of the binding affinity to thrombin of DNA aptamers of various configurations has been performed by the thickness shear mode acoustic method (7) and by electrochemical impedance spectroscopy (28). In addition to the conventional biotinylated single-stranded DNA aptamers (BF), those containing a rigid supporting part formed by a short DNA strand complementary to the BF supporting part (BFA) and aptamer dimers (BFF) were immobilized onto a surface of quartz crystal by the neutravidin-biotin binding method (13) or to a surface of multiwalled carbon nanotubes (28). It has been shown that BFA aptamers revealed higher affinity to thrombin, whereas those of BF and BFF were comparable. This has been explained by improved orientation of BFA aptamers due to the rigid supporting part. The lower binding affinity of BFF in comparison with those of BFA has been elucidated by lower surface concentration of BFF due to bulky symmetrical binding sites of the aptamer homodimer. To obtain more information about the mechanisms of interaction between the previously mentioned aptamers and thrombin, we applied SMFS with the optimized immobilization method allowing attachment of a single molecule at the AFM tip.

MATERIALS AND METHODS

Thrombin from human plasma and all chemicals were purchased from Sigma-Aldrich (Schnellendorf, Germany) of the highest purity available. Acetal polyethylene glycol (PEG) linker as well as aldehyde-PEG-linker was synthesized in our laboratory (29).

Thrombin aptamers were purchased from Thermo Fisher Scientific (Ulm, Germany) being composed of the following oligonucleotide sequences: BFA consists of 5′-GGT TGG TGT GGT TGG $(A)_9(T)_{18}$-3′-BIOTIN (first strand) and 5′-$(A)_{18}$-3′ (second strand), and BFF consists of 5′-GGT TGG TGT GGT TGG $(A)_9(T)_{18}$-3′-BIOTIN (first strand) and 5′-$(A)_{27}$ GGT TGG TGT GGT TGG-3′ (second strand). The adenine sequence $(A)_9$ in both strands of BFF is necessary to provide certain conformational freedom for G-quadruplexes.

Tip functionalization

Silicon nitride tips (MSCT, Veeco Instruments, Dourdan, France) were precleaned by washing thoroughly in chloroform and drying in a gentle stream of nitrogen gas immediately before derivatization. The tips were amino-functionalized using aminopropyltrioxysilane coating according to Ebner et al. (30). A polyethylene glycol (PEG) linker (either NHS-PEG_{18}-aldehyde (31) or NHS-PEG_{18}-acetal (29)) was attached by incubating the tip for 2 h in 3.3 mg/ml (aldehyde) or 1 mg/ml (acetal) PEG linker in chloroform containing 0.5% (v/v) of triethylamine as catalyst. To remove the excess of unbound linker molecules, the tips were washed three times with chloroform and dried in a gentle nitrogen gas stream. In case of NHS-PEG_{18}-acetal the acetal group was inverted into an aldehyde residue by incubation of the tip in 1% v/v citric acid (10 min) followed by washing in water (3 × 5 min). Streptavidin was coupled to the aldehyde residue of the PEG linker by immersing the tips in 0.15 mg/ml streptavidin solution containing 20 mM $NaCNBH_3$ for 1 h. 10 min before the reaction was stopped 5 mM ethanolamine were added to saturate free amino groups.

Afterward, the tips were washed three times in phosphate buffered saline buffer (150 mM NaCl, 5 mM NaH_2PO_4, pH = 7.4) and incubated in 1 μM thrombin-aptamer solution (BFA, BFF) for 1 h at room temperature (RT) (~22°C). Finally, the cantilevers were washed with working buffer (140 mM NaCl, 5 mM KCl, 1 mM $CaCl_2$ $2H_2O$, 1 mM $MgCl_2$ $6H_2O$, 20 mM TRIS, pH = 7.4) and stored in this buffer at 4°C.

Surface preparation

Thrombin was either directly adhered to freshly cleaved mica or coupled via ethylene glycol-bis(succinic acid *N*-hydroxysuccinimide) ester. Using the latter, aminopropyltrioxysilane-coated mica sheets were incubated in ethylene glycol-bis(succinic acid *N*-hydroxysuccinimide) ester (1 mg/ml chloroform) containing 0.5% (v/v) triethylamine for 2 h and extensively washed with chloroform in close analogy to Kamruzzahan et al. (32). For both surface functionalization methods, the thrombin was coupled via incubation of 500 μl 900 nM thrombin solution over night at 4°C until further use. For a surface with a significantly lower thrombin density, 500 μl of 9 nM thrombin solution was incubated over night at 4°C on a cleaved mica surface.

AFM measurements

All AFM measurements were performed in a working buffer using a PicoSPM II setup (Agilent Technologies, Tempe, AZ). Magnetically coated silicon nitride AFM cantilevers (Type VI MACLevers, Agilent Technologies) with a nominal spring constant of 0.292 N/m were used for MAC mode imaging of the thrombin surface. The imaging scan speed was adjusted to 1 line/s at 512 data points/line.

The interaction between certain thrombin aptamers (BFA, BFF) and thrombin was studied by SMFS. Force-distance cycles were recorded at RT using either BFA or BFF functionalized cantilevers (MSCT, Veeco Instruments,) with 0.01 to 0.03 N/m nominal spring constants in the conventional contact force spectroscopy mode. At a fixed lateral position the modified cantilever was approached (trace) toward the thrombin surface and subsequently retracted. The deflection (Δz) of the cantilever from which the force can be directly calculated according to Hook's law ($f = k\Delta z$, k being the cantilever spring constant) was permanently monitored and plotted versus tip-surface separation (i.e., distance). Upon trace, the cantilever bending remained zero. When the aptamer on the tip had bound to a thrombin molecule on the surface, an attractive force developed upon withdrawal causing the cantilever to bend downward. At a critical force, the unbinding force (f_u), the aptamer on the tip was detached from thrombin and the cantilever jumped back to its neutral position.

Dynamic force spectroscopy measurements in which the loading rate r being the product of the pulling velocity v times the effective spring constant k_{eff} was varied and provided insights into the energy landscape of the binding pocket. Thereto, the sweep range was set between 100 and 500 nm with a sweep rate of 0.25–2 Hz, resulting in loading rates from 400 to 40,000 pNs^{-1}. Typically, up to 1000 force-distance cycles were performed for one cantilever carrying a certain thrombin aptamer at a particular loading rate. The spring constants were determined using the thermal noise method to gain a valid force value (33,34). For both aptamer molecules (BFA and BFF) specificity proved experiments were performed by incubating the modified tips with 100 μl 1 μM thrombin for 1–2 h at RT.

Data evaluation

For every individual pulling rate single unbinding events were collected from force-distance cycles. From such unbinding events the rupture force and effective spring constant (slope at rupture) were extracted (35). Empirical probability density functions (pdfs) of the rupture forces were constructed according to Baumgartner et al. (36), allowing to extract the most probable unbinding force (f_u) (35) as a function of the loading rate r. All force distributions of BFF and BFA were fitted against a sum of Gaussians (35):

$$\sum_{1=1}^{N} A_i \frac{1}{\sigma_i\sqrt{2\pi}} \exp\left(-\frac{(x-\mu_i)^2}{2\sigma_i^2} \right), \tag{1}$$

including the boundary condition $\sum_{i=1}^{N} A_i = 1$, taking the probability density property of the pdfs into account, where A_i is a prefactor, μ_i is the position, and σ_i is the width of peak i. For multimodal force distributions the position of the lowest peak was used as f_u. The loading rate was determined by multiplying the pulling speed with the mean effective spring constant. According to Bell (37) and Evans (38) the unbinding force f_u is dependent on the logarithm of the loading rate r through

$$f_u = \frac{k_B T}{x_\beta} \ln\left(\frac{x_\beta r}{k_B T k_{off}} \right), \tag{2}$$

where k_BT is the thermal energy, x_β is the width of the prominent energy barrier from the energy minimum to the energy maximum in the direction of the pulling force, and k_{off} is the dissociation rate constant. The parameters x_β and k_{off} were extracted by fitting Eq. 2 to the experimental data using a generalized least square fitting procedure, which accounts for errors in determining f_u and r (39,40). Our fit procedure used Marquardt's algorithm (41) to solve this problem. The uncertainties in determining the most probable unbinding force was calculated by dividing the standard deviation by the square root of the number of unbinding events and the uncertainties for the loading rate was the pulling rate times the standard deviation of the measured effective spring constants. The uncertainties of the estimated parameters were calculated from the covariance matrix as defined in Jefferys (39).

The loading rate dependence of the second peak of BFF force distribution was described by a Markovian binding model (42,43):

$$r = k_{off} \frac{k_B T}{x_\beta} \left[\sum_{l=1}^{N_B} \frac{1}{l!} \exp\left(-\frac{F^* x_\beta}{l k_B T} \right) \right]^{-1}, \tag{3}$$

where k_{off} and x_β are the above acquired parameters, N_B (= 2) is the number of bindings, and F^* is the most probable unbinding force.

The kinetic off rate constant for contemporaneous rupture of both BFF binding sites was determined to be $k_{off,N_B} = k_{off}[\sum_{l=1}^{N_B}(1/l)]^{-1}$ using the framework of the Markovian binding model (36). All calculations have been done using MATLAB (The MathWorks, Natick, MA).

RESULTS AND DISCUSSION

Immobilization of thrombin and aptamers

DNA aptamers are expected to have a great potential for sensing applications (e.g., AFM force spectroscopy). The sterical conditions for the complex formation are a critical parameter. To obtain the strongest possible complex formation a good orientation and optimal adjusted aptamer density is needed. Different approaches are available to immobilize an aptamer onto an AFM tip (13). Here, we focused on the generation of real single molecule biosensing tips in contrast to previous studies (16,44) where densely packed thiolated aptamers were used yielding weaker interaction forces as a result of sterical hindrance. In addition, we tried to optimize the coupling protocol in points of reproducibility and adaptability. Finally, we want to investigate the ability of

bivalent binding using DNA aptabodies. Tip chemistry based on silanization and pegylation using heterobifunctional cross-linkers was performed to couple a single streptavidin molecule to the outer tip apex. This enables an easy one step binding of all kinds of biotinylated ligands because streptavidin and biotin are known to form a very stable complex. This is especially true if the interaction time exceeds a certain period known to form a tighter interaction between streptavidin and biotin (known as streptavidin-biotin paradox (45)). In this study, we compared two kinds of biotinylated aptamers (see Fig. 1 *B*). BFA (Fig. 1 *B*, *left panel*) contains only one thrombin binding sequence but is equipped with an improved linker part, which is expected to have an enhanced binding behavior toward thrombin compared to conventional single-stranded BF (7,28). As a second type of ligand, BFF (Fig. 1 *B*, *right panel*), a kind of homodimeric double-stranded aptamer, also called aptabody (24), was used. The structure of BFF is expected to perform bivalent binding. Both biotinylated aptamers, BFA and BFF were able to form a tight and long-term stable bond with streptavidin that is tethered to the AFM tip.

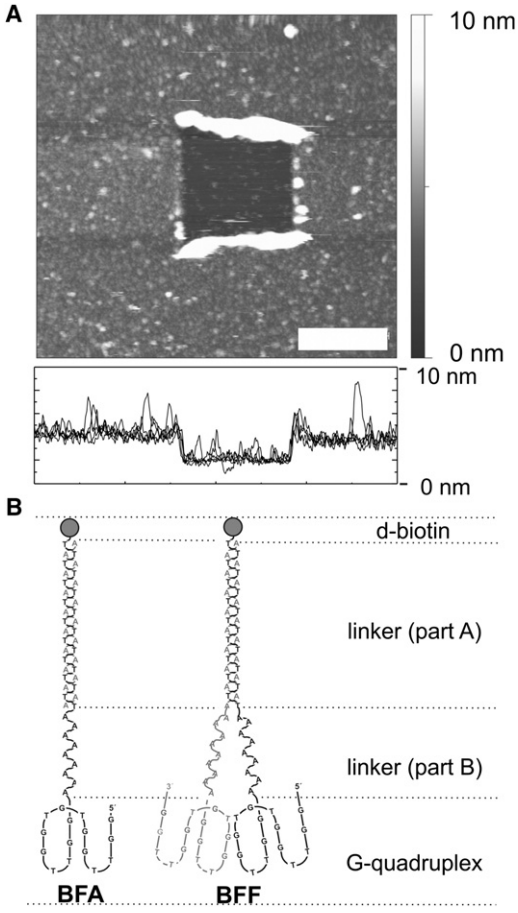

FIGURE 1 Thrombin immobilization. (*A*) Topographical MAC mode image of a dense thrombin monolayer. Image size is 2.0 × 2.0 μm^2. A significantly increased indentation force was applied to remove thrombin molecules from the surface with a square of 500 × 500 nm^2. The overlaid cross-section profiles show a layer height of 2–3 nm. Scale bar length is 500 nm. (*B*) Schematic representation of thrombin aptamers (BFA and BFF) sensitive to fibrinogen binding site of thrombin (see Experimental section).

Thrombin has been bound either covalently or via physisorption to a flat solid support of freshly cleaved mica as described in the Materials and Methods. Although the immobilization method does not allow a site-directed coupling, a statistically dense layer can be generated assuring a sufficient binding probability in SMFS experiments. To prove the quality and density of the thrombin layer, the surface was imaged in dynamic force mode (MAC mode) with low forces. After increasing the force ~5-fold a smaller area of 500 × 500 nm was scanned with lowered feedback gains. Thereby the protein was scratched away. After increasing the scan area to 1 μm^2 a scratched hole with a lack of thrombin molecules could clearly be observed (Fig. 1 *A*). The generated height difference of 2.3 nm reflects the height of the protein layer, which is in accordance with the expected thrombin height (46).

Single molecule force spectroscopy

In so-called force-distance cycles the cantilever containing the generated single molecule biosensing tip (Fig. 2 *A*) approaches the surface until a preset deflection force is reached (*gray line* in Fig. 2 *B*). In the time of contact the tip tethered aptamer ligand can form a complex with the surface bound thrombin. In the retraction period (*black line* in Fig. 2 *B*) a formed ligand-receptor complex becomes ruptured again due to the increasing pulling force. This is observable in the force-distance cycles as an additional (downward) change of the deflection whereby the parabolic shape is a result of the nonlinear spring constant of the linker-ligand/receptor complex. The height of the jump to the resting position directly reflects the unbinding force at a given force loading rate (as described in detail in Materials and Methods). As an outcome, the maximum of the Gaussian peak in the calculated pdf (Fig. 2 *C*) reflects the most probable unbinding force with a higher accuracy compared to a conventional histogram. In the exemplified pdf in Fig. 2 *C* the force pdf of a BFF functionalized tip on a thrombin layer investigated at a loading rate of 1300 pN/s is shown. To distinguish specific aptamer-thrombin interactions from nonspecific adhesion specificity proof experiments are required. For this purpose a so-called tip block experiment was performed. After collecting a set of force-distance cycles with an active biosensor tip, free thrombin molecules are added to the measuring cell resulting in a tip-aptamer-thrombin complex. The sensing tip is thereby inactivated so that no specific complex with the blocked sensor-tip and surface bound thrombin can be formed. This tip block resulted in a significant decrease of the binding probability from 33% (*solid line* in Fig. 2 *C*) to 3.8% (*dashed line* in Fig. 2 *C*) and thereby positively

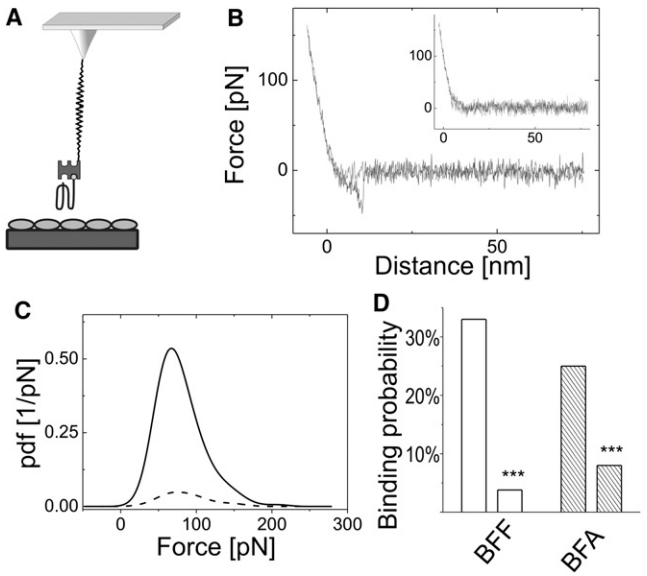

FIGURE 2 Single molecule force spectroscopy experiments. (*A*) The heterobifunctional cross-linker NHS-PEG_{18}-acetal (or NHS-PEG_{18}-aldehyde) was covalently bound to the aminopropyltrioxysilane-coated AFM tip through its NHS-ester function. Streptavidin was attached to the free aldehyde residue (after deprotection of the acetal group). Finally, the biotinylated thrombin-aptamer BFA or BFF was coupled to streptavidin. (*B*) Typical force-distance cycle for the specific interaction between a thrombin-aptamer on the tip and a thrombin molecule on the surface. The parabolic-like shape of the retrace curve (*black line*) corresponds to the dissociation of the bond between thrombin and the BFF aptamer. The specific unbinding events vanished after blocking the aptamer tip by adding free thrombin (*insert*). (*C*) Typical pdf profile of the most probable unbinding force observed for BFF in absence (*solid line*) and presence (*dashed line*) of free thrombin. The highest peak of the Gaussian fit for unblocked condition is found at ~77 pN at a loading rate of 1440 pN/s. (*D*) Binding probability of BFA and BFF before and after tip block with thrombin shown for one representative tip for each aptamer. The number of unbinding events was quite comparable for BFA and BFF.

proved the specificity of the interaction. Although the data shown in Fig. 2, *B* and *C*, are only collected from BFF aptamer, it was proven by the same tip block experiments that all data collected with BFA functionalized tips are also highly specific (Fig. 2 *D*).

By varying the pulling velocity the most probable unbinding forces were measured at different loading rates. For both ligands, BFA and BFF, the most probable unbinding force is increased with an increase of the force loading rate (Fig. 3 *A*). However, fitting of the force distributions of BFF and BFA against a sum of Gaussians (see Materials and Methods) revealed a multimodal binding behavior only in the case of homodimeric BFF (Fig. 3 *B*). In particular, two distinct populations of forces (Fig. 3 *B*, *right panel*) with the second one being a roughly doubled unbinding force were found. The first peak of the BFF force pdf resulted from single binding of one aptamer binding epitope (single binding) with thrombin, whereas the second peak showed the force needed for disrupting the simultaneous binding of both aptamer arms (double binding) to two thrombin molecules. To prove this assumption, we repeated the experiment with a BFF sensor tip on with a significantly reduced surface density of thrombin (Fig. 3 *C*, *left*) to sterically avoid bivalent bindings. As a result, the probability of doubled forces was reduced significantly from 51% on a dense layer to 15% on a layer with low thrombin density. Thus, these results clearly demonstrated that the second force peak of the Gaussian distribution originates from the simultaneous rupture of the two binding epitops of BFF. To explore the energy landscape of the receptor-ligand complex the most probable unbinding force of BFA and BFF was plotted against the logarithm of the loading rate and fitted according to Eq. 2. For double binding of BFF the experimentally obtained data were in good agreement with the expectations of a Markovian binding model (Eq. 3). In particular, the slopes of the partial regression lines in the loading rate dependences of the unbinding forces reflected the energy barrier x_β (Fig. 3 *A*). The resultant x_β values were quite similar for BFA (x_β: 1.73 ± 0.50 Å) and BFF (x_β: 2.21 ± 0.88 Å). However, BFA (k_{off}: 2.84 ± 2.55 s^{-1}) dissociated from thrombin significantly (p-value < 0.05) slower compared to single epitope binding of BFF (k_{off}: 6.61 ± 3.37 s^{-1}), indicating a more proper fitting compared to homodimeric BFF. The dissociation rate, k_{off}, of the contemporaneous rupture of both BFF binding sites determined using the framework of the Markovian binding model (see Materials and Methods) (k_{off}: 4.41 ± 2.25 s^{-1}) was between the BFA and single BFF binding. This outcome is in good agreement with earlier studies on BFA, BFF, and the single-stranded DNA aptamer BF using the thickness shear mode and electrochemical impedance spectroscopy methods (7,28). Due to a successful reduction of sterical hindrance, BFF and BFA show a significantly stronger binding force (up to 20-fold higher) compared to a dense BF functionalized AFM sensor tip (14). The higher rupture force for BFA compared to BFF can be explained by the optimized aptamer orientation due to its rigid supporting part. In addition, BFF measurements showed a second peak in the force pdf at roughly doubled unbinding forces (Fig. 3 *C*, *right panel*) because BFF is an aptabody build up by two thrombin binding DNA sequences. This directly proves, despite certain sterical hindrance, that the second binding site of aptamer dimer (aptabody) is active and binds to the adjacent thrombin molecule. These results are also supported by our recent work on increased anticoagulant activity of BFF dimers in comparison with conventional BF aptamers (26). Moreover, the observed values of the aptamers investigated in this study are nicely comparable to earlier force spectroscopy studies (x_β: 3.2 Å; k_{off}: 2.06 s^{-1}) of Yu et al. (22) working with the same quadruplex DNA structure, but with tetra-thymine on the 5′ and the 3′ end. There they are used as an inverted alignment of ligand and receptor avoiding sterical limitation of an aptamer functionalized tip.

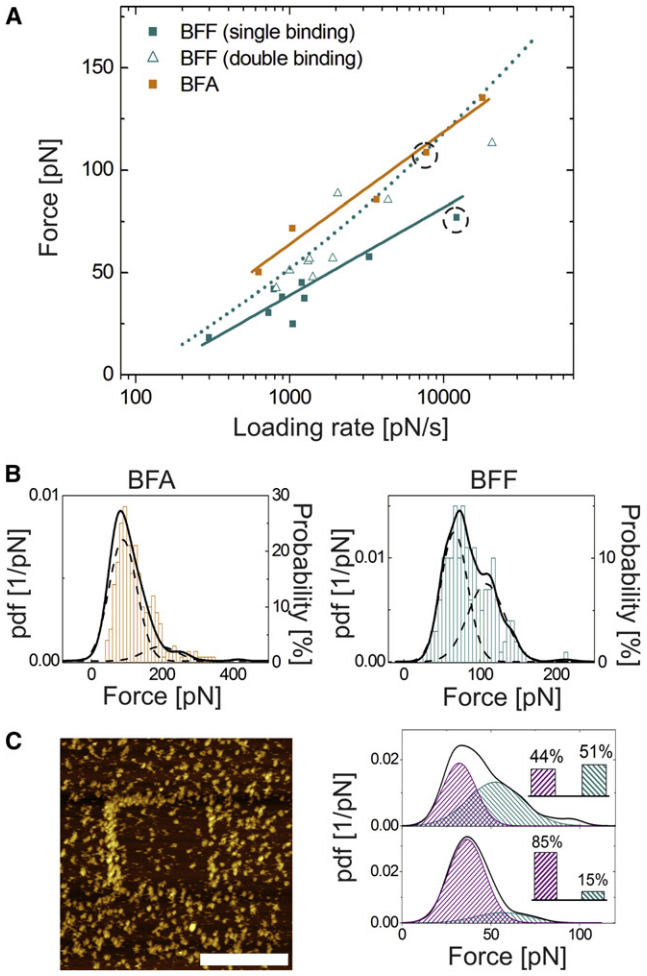

FIGURE 3 Dynamic force spectroscopy measurements. (*A*) Comparison of the dynamic force spectra of BFA and BFF. The most probable unbinding forces were plotted against the logarithm of the loading rate. The lowest forces were found for single binding interaction of BFF (*solid green squares*). The forces of stabilized thrombin-aptamer BFA (*solid orange squares*) were slightly higher compared to those found for double binding of BFF (*open green triangles*). Dynamic force spectroscopy data from BFA and single binding BFF were fitted against Eq. 2. The solid lines represent the acquired fit functions, respectively. Double binding BFF data (*open green triangles*) were in good agreement with the expectations of a Markovian binding model (Eq. 3). BFA revealed the lowest value for dissociation indicating a more proper fitting compared to homodimeric BFF. (*B*) Pdfs of the most probable unbinding forces expressed by a Gaussian fit supplemented with a force histogram for BFA and BFF at comparable loading rates, i.e., ~8900 pN/s for BFA and 14,800 pN/s for BFF (pdfs correspond to the circled data points in (*A*)). The solid line plots in both panels indicate the pdfs built up by the sum of Gaussian fits over all forces. The dashed line plots represent the contributions of the single and double bindings to the distribution fitted by a simple Gaussian function. A prominent second force peak was only obtained in the case of BFF (*dashed lines*). (*C*) Validation of BFF double binding. The left panel shows a representative image of a surface with lower thrombin molecule density that was used to evaluate BFF binding characteristics; scale bar of 300 nm. By applying a higher indentation force the molecules were removed to the outer edges of the scratching area. BFF double binding, which was observed with a high probability on a dense thrombin layer (*upper part in right panel*), was significantly reduced when single thrombin molecules were probed (*lower part in right panel*). The Gaussian fitting procedure to the most probable unbinding forces gained on a dense thrombin layer indicated a probability of 44% for the occurrence of a single binding and 51% for the occurrence of a double binding (*upper part of the right panel*). In contrast thereto, the single binding occurrence was increased to 85% on single thrombin molecules, whereas the double binding occurrence was lowered to 15% (*lower part of left panel*).

CONCLUSION

In conclusion, within this study we could clearly demonstrate a simple but effective strategy to bind biotinylated aptamers to previously PEG-streptavidin functionalized tips in a one step reaction. Changes in the sterical behavior of the linker part of the thrombin aptamer increases the aptamer thrombin complex stability, resulting in a lower k_{off} value. This allows use of the full potential of DNA aptamers for biosensing techniques such as molecular recognition force spectroscopy and recognition imaging. In addition, we demonstrated the high efficiency of bivalent binding of DNA aptabodies. Because the use of DNA aptamers is increasing significantly, this outcome will help to enhance the potential of aptamers and to simplify the characterization on the real single molecule level.

SUPPORTING MATERIAL

A figure is available at http://www.biophysj.org/biophysj/supplemental/S0006-3495(11)00953-2.

The authors thank Dr. Hermann Gruber, Dr. Linda Wildling, and Dr. Barbara Unterauer for their support regarding heterobifunctional cross-linker synthesis.

This work was financially supported by the Micro-Nano-Technology (MNT)-ERA.NET project IntelliTip, by the FFG (project 823980) and by the Slovak Academy of Sciences (ID 431, grant agreement No. 234989), and by the Finnish Funding Agency for Technology and Innovation (TEKES). Financial support from the Slovak Research and Development Agency under contract No. APVV-0410-10 is gratefully acknowledged.

REFERENCES

1. Ellington, A. D., and J. W. Szostak. 1990. In vitro selection of RNA molecules that bind specific ligands. *Nature.* 346:818–822.
2. Hianik, T., and J. Wang. 2009. Electrochemical aptasensors-recent achievements and perspectives. *Electroanalysis.* 21:1223–1235.
3. Farokhzad, O. C., S. Jon, …, R. Langer. 2004. Nanoparticle-aptamer bioconjugates: a new approach for targeting prostate cancer cells. *Cancer Res.* 64:7668–7672.
4. Holland, C. A., A. T. Henry, …, F. C. Church. 2000. Effect of oligodeoxynucleotide thrombin aptamer on thrombin inhibition by heparin cofactor II and antithrombin. *FEBS Lett.* 484:87–91.
5. Bock, L. C., L. C. Griffin, …, J. J. Toole. 1992. Selection of single-stranded DNA molecules that bind and inhibit human thrombin. *Nature.* 355:564–566.
6. Schultze, P., R. F. Macaya, and J. Feigon. 1994. Three-dimensional solution structure of the thrombin-binding DNA aptamer d(GGTTGGTGTGGTTGG). *J. Mol. Biol.* 235:1532–1547.
7. Hianik, T., I. Grman, and I. Karpisova. 2009. The effect of DNA aptamer configuration on the sensitivity of detection thrombin at surface by acoustic method. *Chem. Commun. (Camb.).* (41):6303–6305.

8. Lee, G. U., D. A. Kidwell, and R. J. Colton. 1994. Sensing discrete streptavidin-biotin interactions with atomic force microscopy. *Langmuir.* 10:354–357.
9. Florin, E. L., V. T. Moy, and H. E. Gaub. 1994. Adhesion forces between individual ligand-receptor pairs. *Science.* 264:415–417.
10. Hinterdorfer, P., W. Baumgartner, …, H. Schindler. 1996. Detection and localization of individual antibody-antigen recognition events by atomic force microscopy. *Proc. Natl. Acad. Sci. USA.* 93:3477–3481.
11. Ebner, A., R. Nevo, …, P. Hinterdorfer. 2009. Probing the energy landscape of protein-binding reactions by dynamic force spectroscopy. *In* Handbook of Single-Molecule Biophysics. P. Hinterdorfer and A. Van Oijen, editors. Springer, New York. 407–447.
12. Kienberger, F., A. Ebner, …, P. Hinterdorfer. 2006. Molecular recognition imaging and force spectroscopy of single biomolecules. *Acc. Chem. Res.* 39:29–36.
13. Ebner, A., L. Wildling, …, H. J. Gruber. 2008. Functionalization of probe tips and supports for single-molecule recognition force microscopy. *Top. Curr. Chem.* 285:29–76.
14. Dammer, U., M. Hegner, …, H. J. Güntherodt. 1996. Specific antigen/antibody interactions measured by force microscopy. *Biophys. J.* 70:2437–2441.
15. Ros, R., F. Schwesinger, …, L. Tiefenauer. 1998. Antigen binding forces of individually addressed single-chain Fv antibody molecules. *Proc. Natl. Acad. Sci. USA.* 95:7402–7405.
16. Basnar, B., R. Elnathan, and I. Willner. 2006. Following aptamer-thrombin binding by force measurements. *Anal. Chem.* 78:3638–3642.
17. Miyachi, Y., N. Shimizu, C. Ogino, and A. Kondo. 2010. Selection of DNA aptamers using atomic force microscopy. *Nucleic Acids Res.* 38:21–28.
18. Lin, L., H. Wang, …, S. Lindsay. 2006. Recognition imaging with a DNA aptamer. *Biophys. J.* 90:4236–4238.
19. Eckel, R., S. D. Wilking, …, D. Anselmetti. 2005. Single-molecule experiments in synthetic biology: an approach to the affinity ranking of DNA-binding peptides. *Angew. Chem. Int. Ed. Engl.* 44:3921–3924.
20. Baumgarth, B., F. W. Bartels, …, R. Ros. 2005. Detailed studies of the binding mechanism of the *Sinorhizobium meliloti* transcriptional activator ExpG to DNA. *Microbiology.* 151:259–268.
21. Bartels, F. W., B. Baumgarth, …, A. Becker. 2003. Specific binding of the regulatory protein ExpG to promoter regions of the galactoglucan biosynthesis gene cluster of *Sinorhizobium meliloti*—a combined molecular biology and force spectroscopy investigation. *J. Struct. Biol.* 143:145–152.
22. Yu, J., Y. Jiang, …, X. Fang. 2007. Energy landscape of aptamer/protein complexes studied by single-molecule force spectroscopy. *Chem. Asian J.* 2:284–289.
23. Hasegawa, H., K. Taira, …, K. Ikebukuro. 2008. Improvement of aptamer affinity by dimerization. *Sensors.* 8:1090–1098.
24. Hianik, T., A. Porfireva, …, G. Evtugyn. 2008. Aptabodies - new type of artificial receptors for detection proteins. *Protein Pept. Lett.* 15: 799–805.
25. Di Giusto, D. A., and G. C. King. 2004. Construction, stability, and activity of multivalent circular anticoagulant aptamers. *J. Biol. Chem.* 279:46483–46489.
26. Poniková, S., K. Tlučková, …, T. Hianik. 2011. The circular dichroism and differential scanning calorimetry study of the properties of DNA aptamer dimers. *Biophys. Chem.* 155:29–35.
27. Michalowski, D., R. Chitima-Matsiga, …, D. H. Burke. 2008. Novel bimodular DNA aptamers with guanosine quadruplexes inhibit phylogenetically diverse HIV-1 reverse transcriptases. *Nucleic Acids Res.* 36:7124–7135.
28. Porfireva, A. V., G. A. Evtugyn, …, T. Hianik. 2010. Impedimetric aptasensors based on carbon nanotubes-poly (methylene blue) composite. *Electroanalysis.* 22:2187–2195.
29. Wildling, L., B. Unterauer, …, H. J. Gruber. 2011. Linking of sensor molecules with amino groups to amino-functionalized AFM tips. *Bioconjug. Chem.* 22:1239–1248.
30. Ebner, A., P. Hinterdorfer, and H. J. Gruber. 2007. Comparison of different aminofunctionalization strategies for attachment of single antibodies to AFM cantilevers. *Ultramicroscopy.* 107:922–927.
31. Ebner, A., L. Wildling, …, H. J. Gruber. 2007. A new, simple method for linking of antibodies to atomic force microscopy tips. *Bioconjug. Chem.* 18:1176–1184.
32. Kamruzzahan, A. S. M., F. Kienberger, …, P. Hinterdorfer. 2004. Imaging morphological details and pathological differences of red blood cells using tapping-mode AFM. *Biol. Chem.* 385:955–960.
33. Butt, H. J., M. Jaschke, and W. Ducker. 1995. Measuring surface forces in aqueous electrolyte solution with the atomic force microscope. *Bioelectrochem. Bioenerg.* 38:191–201.
34. Hutter, J. L., and J. Bechhoefer. 1993. Calibration of atomic-force microscope tips. *Rev. Sci. Instrum.* 64:1868–1873.
35. Rankl, C., F. Kienberger, …, P. Hinterdorfer. 2007. Accuracy estimation in force spectroscopy experiments. *Jpn. J. Appl. Phys.* 46:5536–5539.
36. Baumgartner, W., P. Hinterdorfer, and H. Schindler. 2000. Data analysis of interaction forces measured with the atomic force microscope. *Ultramicroscopy.* 82:85–95.
37. Bell, G. I. 1978. Models for the specific adhesion of cells to cells. *Science.* 200:618–627.
38. Evans, E., and K. Ritchie. 1997. Dynamic strength of molecular adhesion bonds. *Biophys. J.* 72:1541–1555.
39. Jefferys, W. H. 1990. On the method of least squares. *Astron. J.* 85: 177–181.
40. Lybanon, M. 1984. A better least-squares method when both variables have uncertainties. *Am. J. Phys.* 52:22–26.
41. Jefferys, W. H. 1981. On the method of least squares-part two. *Astron. J.* 86:149–155.
42. Rankl, C., F. Kienberger, …, P. Hinterdorfer. 2008. Multiple receptors involved in human rhinovirus attachment to live cells. *Proc. Natl. Acad. Sci. USA.* 105:17778–17783.
43. Williams, P. M. 2003. Analytical descriptions of dynamic force spectroscopy: behaviour of multiple connections. *Anal. Chim. Acta.* 479:107–115.
44. Zhang, X., and V. K. Yadavalli. 2010. Molecular interaction studies of vascular endothelial growth factor with RNA aptamers. *Analyst (Lond.).* 135:2014–2021.
45. Pincet, F., and J. Husson. 2005. The solution to the streptavidin-biotin paradox: the influence of history on the strength of single molecular bonds. *Biophys. J.* 89:4374–4381.
46. Pechik, I., J. Madrazo, …, L. Medved. 2004. Crystal structure of the complex between thrombin and the central "E" region of fibrin. *Proc. Natl. Acad. Sci. USA.* 101:2718–2723.